Marine Geology 395 (2018) 65–81

Contents lists available at ScienceDirect

Marine Geology

journal homepage: www.elsevier.com/locate/margo

# Assessing climate change impacts on the stability of small tidal inlets: Part 2 - Data rich environments

Trang Minh Duong[a,b], Roshanka Ranasinghe[a,b,c,*], Marcus Thatcher[d], Sarith Mahanama[e,f], Zheng Bing Wang[b], Pushpa Kumara Dissanayake[g], Mark Hemer[h], Arjen Luijendijk[b], Janaka Bamunawala[a], Dano Roelvink[a,b], Dirkjan Walstra[b]

[a] Department of Water Science and Engineering, UNESCO-IHE, PO Box 3015, 2601 DA Delft, The Netherlands
[b] Deltares, PO Box 177, 2600 MH Delft, The Netherlands
[c] Water Engineering and Management, Faculty of Engineering Technology, University of Twente, PO Box 217, 7500 AE Enschede, The Netherlands
[d] CSIRO Oceans & Atmosphere, Private Bag 1, Aspendale, VIC 3195, Australia
[e] Global Modeling and Assimilation Office, NASA Goddard Space Flight Center, Greenbelt, MD, USA
[f] Science Systems and Applications Inc, Lanham, MD, USA
[g] Environmental Physics group, Limnological Institute, University of Konstanz, 78464 Konstanz, Germany
[h] CSIRO Oceans & Atmosphere, GPO Box 1538, Hobart, TAS 7001, Australia

ARTICLE INFO

*Keywords:*
Tidal inlets
Climate change
Numerical modelling
Delft3D
Sri Lanka
Data rich environments

ABSTRACT

Climate change (CC) is likely to affect the thousands of bar-built or barrier estuaries (here referred to as Small tidal inlets - STIs) around the world. Any such CC impacts on the stability of STIs, which governs the dynamics of STIs as well as that of the inlet-adjacent coastline, can result in significant socio-economic consequences due to the heavy human utilisation of these systems and their surrounds. This article demonstrates the application of a process based snap-shot modelling approach, using the coastal morphodynamic model *Delft3D*, to 3 case study sites representing the 3 main STI types; Permanently open, locationally stable inlets (Type 1), Permanently open, alongshore migrating inlets (Type 2) and Seasonally/Intermittently open, locationally stable inlets (Type 3). The 3 case study sites (Negombo lagoon – Type 1, Kalutara lagoon – Type 2, and Maha Oya river – Type 3) are all located along the southwest coast of Sri Lanka.

After successful hydrodynamic and morphodynamic model validation at the 3 case study sites, CC impact assessment are undertaken for a high end greenhouse gas emission scenario. Future CC modified wave and riverflow conditions are derived from a regional scale application of spectral wave models (WaveWatch III and SWAN) and catchment scale applications of a hydrologic model (CLSM) respectively, both of which are forced with IPCC Global Climate Model output dynamically downscaled to ~50 km resolution over the study area with the stretched grid Conformal Cubic Atmospheric Model CCAM. Results show that while all 3 case study STIs will experience significant CC driven variations in their level of stability, none of them will change Type by the year 2100. Specifically, the level of stability of the Type 1 inlet will decrease from 'Good' to 'Fair to poor' by 2100, while the level of (locational) stability of the Type 2 inlet will also decrease with a doubling of the annual migration distance. Conversely, the stability of the Type 3 inlet will increase, with the time till inlet closure increasing by ~75%. The main contributor to the overall CC effect on the stability of all 3 STIs is CC driven variations in wave conditions and resulting changes in longshore sediment transport; not Sea level rise as commonly believed.

## 1. Introduction

Bar-built or barrier estuaries (here referred to as Small tidal inlets - STIs) are one of the 3 main types of inlet-estuary/lagoon systems identified by Bruun and Gerritsen (1960). These systems are commonly found in wave dominated and microtidal environments; especially in tropical and sub-tropical regions of the world (e.g. India, Sri Lanka, Vietnam, Florida (USA), South America (Brazil), South Africa, and SW/SE Australia). STIs generally comprise narrow (< 500 m wide) inlet channels and shallow (average depth < 10 m) estuaries/lagoons with surface areas less than 50 $km^2$ (Duong et al., 2016).

STIs can be classified into 3 main categories based on their general

* Corresponding author at: Department of Water Science and Engineering, UNESCO-IHE, PO Box 3015, 2601 DA Delft, The Netherlands.
*E-mail addresses:* T.Duong@un-ihe.org (T.M. Duong), R.Ranasinghe@un-ihe.org (R. Ranasinghe).

http://dx.doi.org/10.1016/j.margeo.2017.09.007
Received 27 April 2016; Received in revised form 10 September 2017; Accepted 15 September 2017
Available online 22 September 2017

morphodynamic behaviour as:

- Permanently open, locationally stable inlets (Type 1)
- Permanently open, alongshore migrating inlets (Type 2)
- Seasonally/Intermittently open, locationally stable inlets (Type 3).

The Type of the STI reflects the stability of the inlet (i.e. open, close, migrating) which governs the dynamics of the adjacent coastline and of the estuary/lagoon connected to the inlet, and is therefore a key diagnostic in assessing potential CC impacts on STIs. The term "inlet stability", in general usage, may refer to locational stability or channel cross-sectional stability. Locationally stable inlets are those that stay fixed in one location, but may stay open (i.e. locationally and cross-sectionally stable inlets - Type 1) or close intermittently/seasonally (i.e. locationally stable but cross-sectionally unstable inlets - Type 3). Cross-sectionally stable inlets are those in which the inlet dimensions will remain mostly constant over time. However, cross-sectionally stable inlets may also migrate alongshore (i.e. cross-sectionally stable but locationally unstable - Type 2) (Duong et al., 2016).

The stability of STIs (or the inlet condition) is governed by two main phenomena: the flow through the inlet (tidal prism and riverflow) and nearshore sediment transport in the vicinity of the inlet. Thus, inlet stability is a function of the balance between terrestrial (e.g. riverflow) and oceanic forcing (e.g. mean sea level, waves) (Ranasinghe et al., 2013). All of these system forcings are expected to be affected by climate change (CC) (Duong et al., 2016; Ranasinghe, 2016). IPCC (2013) projections indicate a global mean sea level rise (SLR) of 0.26–0.82 m by 2081–2100 (relative to 1986–2005) with the most pessimistic RCP 8.5 scenario projecting an SLR of 0.52 m to 0.98 m by 2081–2100. Where future riverflows are concerned, IPCC (2013) projections for the RCP 8.5 scenario indicate increases/decreases of up to 30% in annual runoff in many parts of the world by the end of the 21st century relative to the present. Hemer et al. (2013) presented wave projections which indicate that annual mean wave heights will decrease in around 25% of the global ocean, while an increase is projected for about 7.1% of the global ocean. Furthermore, Hemer et al. (2013) projected clockwise and anti-clockwise rotations in wave direction for about 40% of the global ocean. Thus, the stability of thousands of STIs around the world that are governed by these forcings are likely to be impacted by CC in the 21st century, potentially resulting in serious socio-economic consequences owing to the wide range of economic activities (e.g. tourist hotels and tourism associated recreational activities, inland fisheries, harbouring of sea going fishing vessels) that STIs and surrounding areas often support.

Recognising the difficulty associated with investigating CC impacts on the stability of STIs via a straightforward application (i.e. a single 100 yearlong morphodynamic simulation) of presently available process based coastal morphodynamic models (e.g. *Delft3D*, *CMS*, *Mike21*, *Xbeach*) (see for e.g. Nienhuis et al., 2016; Dodet et al., 2013;), Duong et al. (2016) proposed two different 'snap-shot' process based modelling approaches to investigate this phenomenon in data poor and data rich environments (see Figs. 10–12 in Duong et al., 2016). The main differences between the two approaches are: (a) the data poor approach uses schematised system bathymetry while the data rich approach requires good measured system bathymetry for model initialisation; (b) the data poor approach uses freely available coarse resolution (~100–200 km) global scale projections of future CC modified system forcing (i.e. waves, riverflows and sea level rise) while the data rich approach requires site specific projections of future system forcing obtained from high resolution regional scale hydrologic and wave models forced with dynamically downscaled Global climate model (GCM) output; and (c) coastal impact models are only qualitatively validated in the data poor approach, while both quantitative and qualitative model validation are required in the data rich approach.

Duong et al. (2017) demonstrates the application of the 'data poor' approach to 3 case study sites representative of the 3 main STI types. This article demonstrates the application of the 'data rich' approach at the same 3 case study sites to derive site-specific projections of CC impacts, and through a comparison of results obtained using the 'data rich' and 'data poor' approaches, suggests a basic guideline on when to use which approach.

## 2. Study areas

The 3 case study sites selected for this study are: Negombo lagoon (Type 1), Kalutara lagoon (Type 2) and Maha Oya river (Type 3), all of which are located along the SW coast of Sri Lanka. For CC impact studies, a study area may be considered to be 'data rich' when wave, wind and riverflow data (ideally exceeding 10 years to encapsulate inter-annual variability); downscaled future CC modified wave and riverflow data, and bathymetries of the study area are available. All these data are available for the 3 case study sites.

Located in the Indian Ocean Southeast of India (Fig. 1), Sri Lanka experiences a tropical monsoon climate with 2 monsoon seasons: the Northeast (NE) monsoon (November–February) and the Southwest (SW) monsoon (May–September). October to December is the wettest period with about one third of the total annual rainfall occurring during this time (Zubair and Chandimala, 2006). The coastal environment of Sri Lanka is micro-tidal (mean tidal range ~0.5 m) and wave dominated (average offshore significant wave height ~1.1 m). The SW coast of Sri Lanka, where the 3 case study sites are located, experiences the most energetic wave conditions during the SW monsoon with offshore significant wave heights of 1–2 m incident from the SW-W octant. Almost all the beaches around the country are sandy with grain diameters ($D_{50}$) of 0.2–0.45 mm. Detailed descriptions of the 3 case study sites are provided in Duong et al. (2017) and are therefore not repeated here. For the sake of completeness however study area locations, case study sites and main system characteristics are shown in Figs. 1, 2 and Table 1 respectively. The system characteristics listed in Table 1 were obtained from a range of sources including scientific articles, technical reports, post-graduate theses, field visits and local experts. Information on Negombo lagoon was mostly obtained from Chandramohan and Nayak (1990) and University of Moratuwa (2003); on Kalutara lagoon from Perera (1993) and GTZ (1994); and on Maha Oya from GTZ (1994). Fluvial sediment transport into the 3 systems is expected to be practically zero due to impoundments at upstream dams (personal communication, Sri Lanka Coast conservation department).

## 3. Methodology

As proposed by Duong et al. (2016) for data rich environments, a modified version of the ensemble modelling framework proposed by Ranasinghe (2016) (Fig. 3) was adopted in this study. Ranasinghe's (2016) modelling framework proposes the sequential application of GCM projections, Regional Climate Models (RCMs), Regional wave/hydrodynamic/catchment models, local wave models, and coastal impact models to obtain a number of different projections of the coastal CC impact of interest.

In Step 5 of the above framework (see Fig. 3), it is necessary to use a coastal impact model that is appropriate for investigating the CC impact of interest. In this study, which focusses on CC impacts on the stability of STIs, the coastal area morphodynamic model *Delft3D* was extensively used (in 2DH mode). The *Delft3D* model is described in detail by Lesser et al. (2004) and hence only a very brief description is provided here. The basic model structure is shown in Fig. 4. The model comprises a short wave driver (SWAN), a 2DH flow module, a sediment transport model (van Rijn, 1993), and a bed level update scheme that communicate with each other during a simulation. To accelerate morphodynamic computations, *Delft3D* adopts the MORFAC approach (Roelvink, 2006; Ranasinghe et al., 2011) which takes into account that time scales associated with bed level changes are generally much greater than those associated with hydrodynamic forcing. The MORFAC approach essentially multiplies the bed levels computed after each hydrodynamic time step by a time varying or constant factor (MORFAC) which results in fast morphodynamic computations.

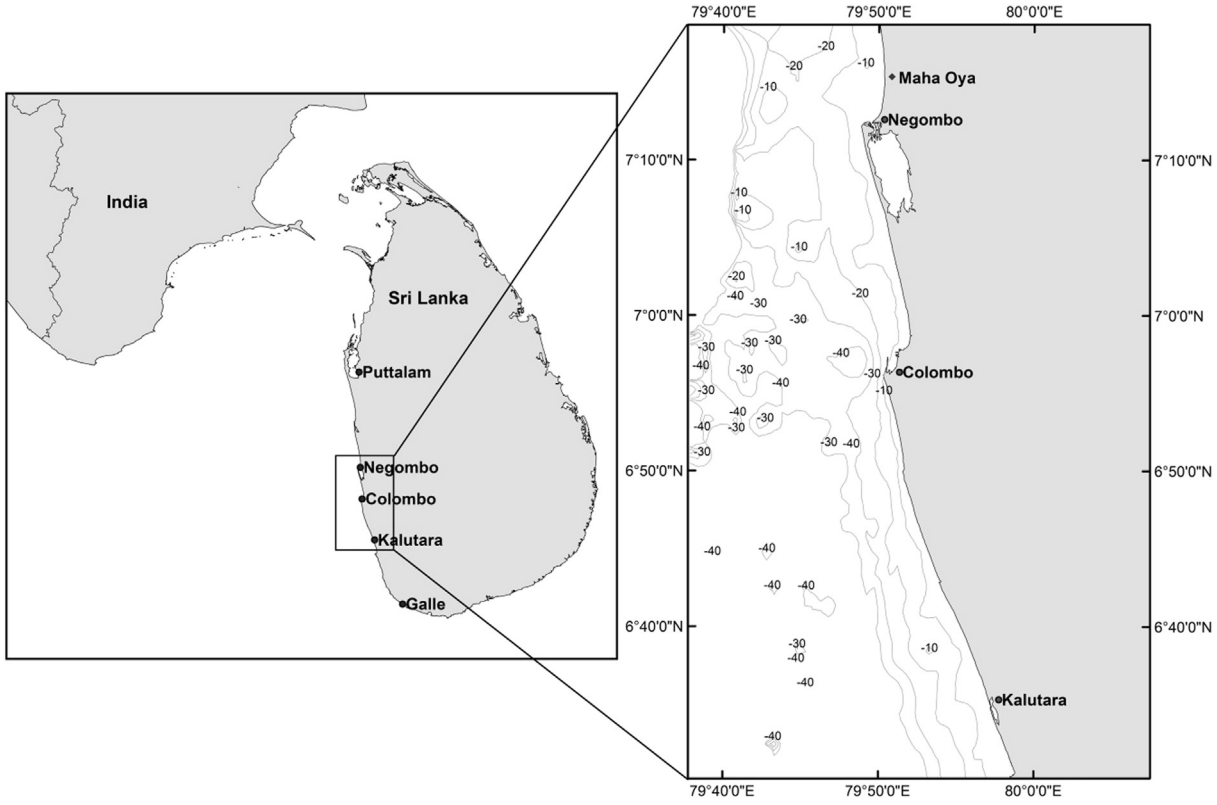


**Fig. 1.** Location of Sri Lanka (left) and the 3 case study sites (right). The location of the Capital city Colombo is also shown for reference. (From Duong et al., 2017.)

CC impact assessment using *Delft3D* as the coastal impact model was done here following the 'snap-shot' approach proposed by Duong et al. (2016) for data rich areas (see Fig. 5). Here, *Delft3D* was first validated using measured hydrodynamic data (i.e. measured water level and velocities within the STI systems). Morphodynamic validation was achieved by performing 'present simulations – PS' of *Delft3D* (up to one year long) forced with measured riverflows and wave conditions, the results of which were compared with observed/reported general inlet behavioural characteristics and annual longshore sediment transport rates. The target of model validations performed in this way was to gain confidence in the model's ability to simulate system morphodynamics by reproducing the contemporary morphodynamic behaviour of the system (e.g. closed/open, locationally stable/migrating). Note that the morphodynamic hindcasts obtained in the PS's were only qualitatively validated in this study as repeated bathymetric data were unavailable for the case study sites. Unfortunately availability of repeated bathymetric data is a rare occurrence around the world and hence, in most situations the best that can be hoped for in CC impact studies of this nature is qualitative morphodynamic validation as done here.

The validated model was then forced with dynamically downscaled CC forcing (at the end of the 21st century) to obtain projections of the system behaviour that can be expected by 2100. Dynamic downscaling

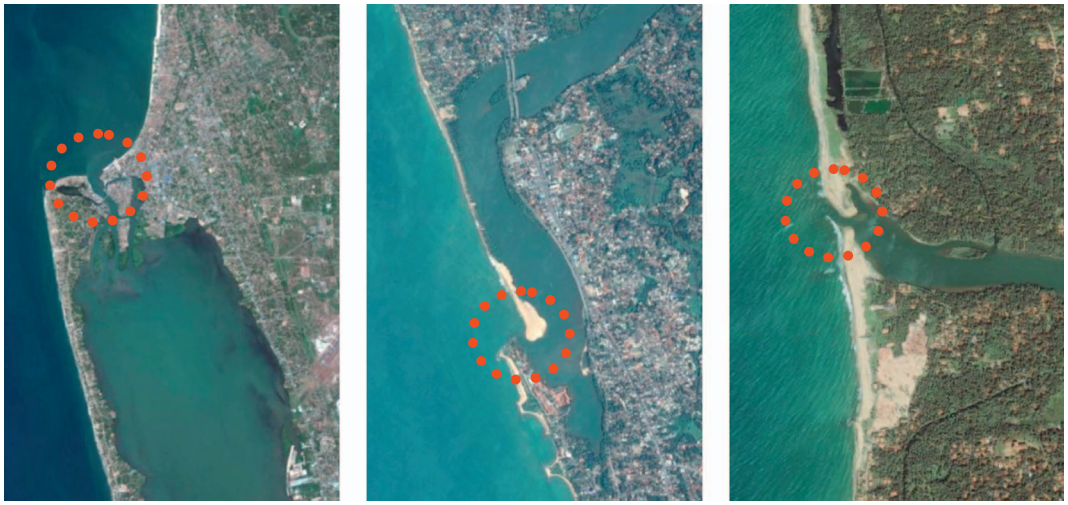

**Fig. 2.** Negombo lagoon - permanently open, locationally stable inlet: Type 1 (left), Kalutara lagoon - permanently open, alongshore migrating inlet: Type 2 (middle), Maha Oya river - seasonally/intermittently open, locationally stable inlet: Type 3 (right). The red dotted circles indicate inlet location. (From Duong et al., 2017). (For interpretation of the references to color in this figure legend, the reader is referred to the web version of this article.)

**Table 1**
Key characteristics of the 3 case study STIs.

| STI system | Inlet dimensions | | | Estuary/lagoon characteristics | | | Coastal characteristics | |
|---|---|---|---|---|---|---|---|---|
| | Width (m) | Length (m) | Depth (m) | Basin area ($km^2$) | Average depth (m) | Riverflow ($Mm^3$/yr) | $D_{50}$ (μm) | Longshore transport ($Mm^3$/yr) |
| Negombo lagoon | 400 | 300 | 3 | 45 | 1 | 2762 | 250 | 0.02 |
| Kalutara lagoon | 150 | 150 | 4.5 | 1.75 | 3 | 7500 | 250 | 0.5 |
| Maha Oya river | 100 | 70 | 3 | 0.2 | 3.5 | 1571 | 250 | 0.5 |

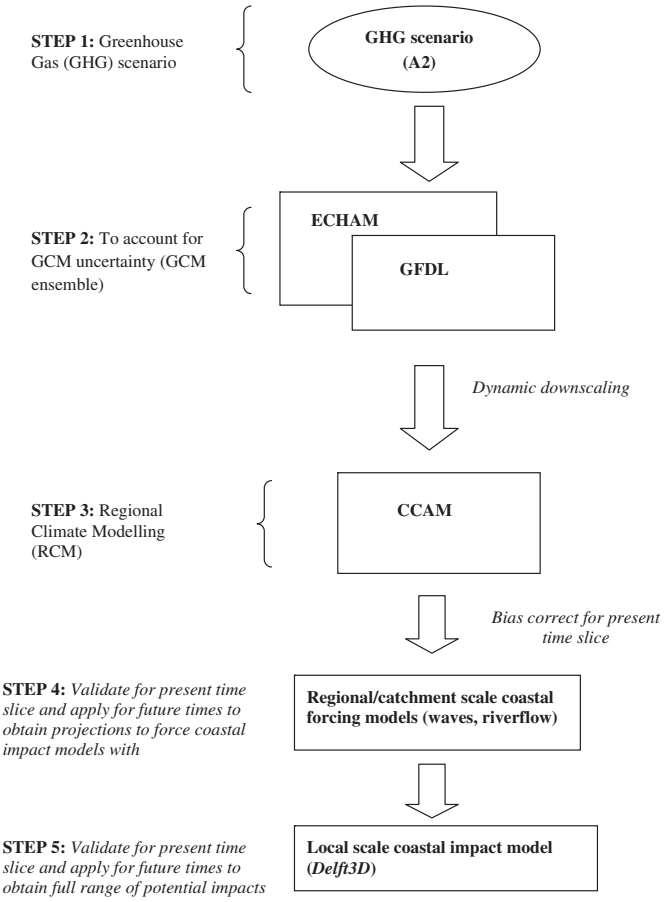


**Fig. 3.** Modelling framework adopted in the present study following the comprehensive ensemble modelling framework proposed by Ranasinghe (2016).

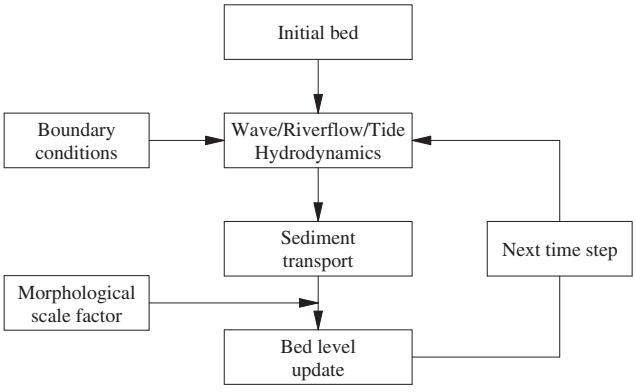


**Fig. 4.** *Delft3D* model structure.

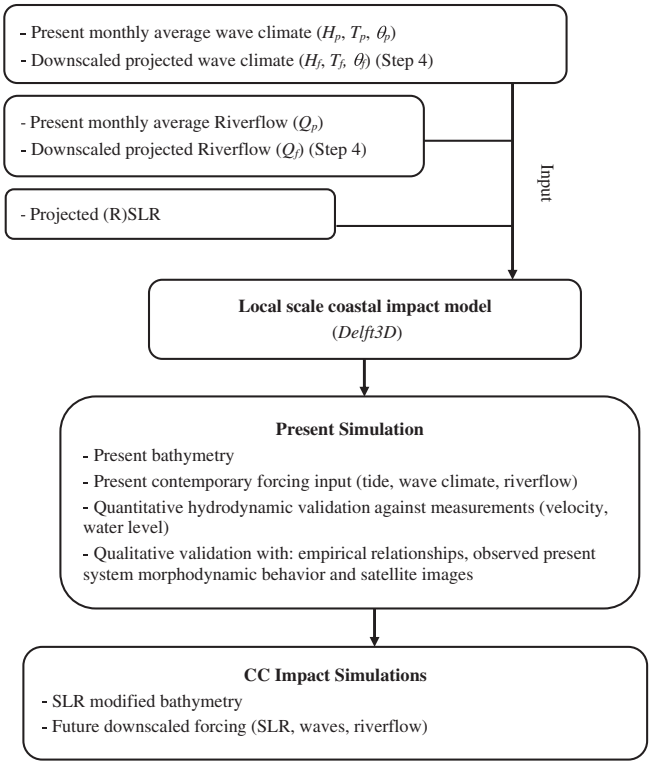


**Fig. 5.** Schematic illustration of the modelling approach for CC impact assessment at STIs in data rich environments. Subscripts '*p*' and '*f*' refer to 'present' and 'future' respectively. (From Duong et al., 2016.)

of GCM derived climate variables is necessary to derive appropriate model forcing for reliable local scale applications of coastal impact models because GCM outputs are generally available at about 1° resolution, which is too coarse for direct application as forcing in local scale impact models. The CC forced snap-shot simulations were also undertaken for the same duration as the PS in each system (except for the intermittently closing Maha Oya river, where the simulations were continued till inlet closure occurred). In simulations incorporating sea level rise (SLR), the slow continuous raising of estuary/lagoon bed level due to the process of 'basin infilling' was taken into account by adjusting the initial bathymetry of the CC snap-shot simulations. Basin infilling is a process that occurs when SLR increases the estuary/lagoon (or basin) volume below mean water level (i.e. 'accommodation space'). Because the basin always strives to maintain a certain equilibrium volume (Stive et al., 1998; Ranasinghe et al., 2013), when this volume is increased due to SLR (or land subsidence) basin hypsometry will change, triggering sediment importation into the basin by wave and tide driven currents to raise the basin bed level. Equilibrium will be reinstated when a sand volume equal to the SLR induced accommodation space (SLR x surface area of basin) is imported into the basin. Stive et al. (1998), however, noted that in most situations there will be a lag between the rate of SLR and basin infilling due to the difference in time

scales associated with hydrodynamic forcing and morphological response. Ranasinghe et al. (2013) showed that, for STIs, this lag is about 0.5 over the 21st century (i.e. basin infill volume = 0.5 × SLR driven increase in accommodation space). In the CC snap-shot simulations involving SLR, the basin infill volume thus calculated was distributed in the lagoon area such that the shape of contemporary basin hypsometry curve was preserved (see Section 5.2). Note that, as upstream dams are thought to completely block all fluvial sediment transport into the 3 case study systems, future fluvial sediment transport into these systems was also assumed to be insignificant.

Throughout this article, the extended inlet behaviour classification scheme proposed by Duong et al. (2017) is used to discuss model results, and hence it is reproduced below in Table 2 for convenience. This classification scheme extends Bruun's (1978) inlet stability classification scheme, which originally linked the ratio ($r$) between tidal prism ($P$) and annual longshore sediment transport ($M$) with inlet stability condition (e.g. good, fair, poor), by making an additional connection between those parameters and the 3 different STI Types mentioned in Section 1 (e.g. permanently open, locationally stable inlets (Type 1); permanently open, alongshore migrating inlets (Type 2); and seasonally/intermittently open, locationally stable inlets (Type 3)).

**Table 2**
Extended classification scheme for inlet Type and stability conditions. (From Duong et al., 2017.)

| Inlet type | $r = P/M$ | Bruun classification |
|---|---|---|
| Type 1 | > 150 | Good |
| | 100 – 150 | Fair |
| | 50 – 100 | Fair to poor |
| | 20 – 50 | Poor |
| Type 2 | 10 – 20 | Unstable (open and migrating) |
| Type 2/3 | 5 – 10 | Unstable (migrating or intermittently closing) |
| Type 3 | 0 – 5 | Unstable (intermittently closing) |

$r$ = Bruun's inlet stability criterion, $P$ = tidal prism ($m^3$), $M$ = annual longshore sediment transport volume ($m^3$).

## 4. Implementation

### 4.1. Dynamic downscaling

As mentioned above, IPCC GCMs generally operate at a grid resolution of about 1°. However, local scale (< 10 km) coastal CC impacts studies require model forcing data at much finer resolution (Ranasinghe, 2016). Therefore, as indicated in the modelling framework for coastal CC impact assessment shown in Fig. 3, GCM outputs first have to be dynamically or statistically downscaled, usually to about 50 km spatial resolution, and subsequently the downscaled climate forcing needs to be used in regional/catchment scale coastal forcing models to obtain the high resolution forcing data that are suitable to use with the coastal impact model (e.g. *Delft3D*). In this study, all downscaled climate variables were derived from the stretched grid model CCAM (Conformal Cubic Atmospheric Model). CCAM is a semi-implicit, semi-Lagrangian atmospheric climate model based on a conformal cubic grid (McGregor and Dix, 2008). Although CCAM is a global atmospheric model, it allows a variable resolution grid which enables a finer grid resolution over the target area at the expense of a coarser resolution on the opposite side of the globe. In this way, CCAM can be used for regional climate experiments without imposing lateral boundary conditions. The variable resolution grid used to derive the downscaled climate variables over Sri Lanka for this study is shown in Fig. 6. In this application, CCAM employed 18 vertical levels (ranging

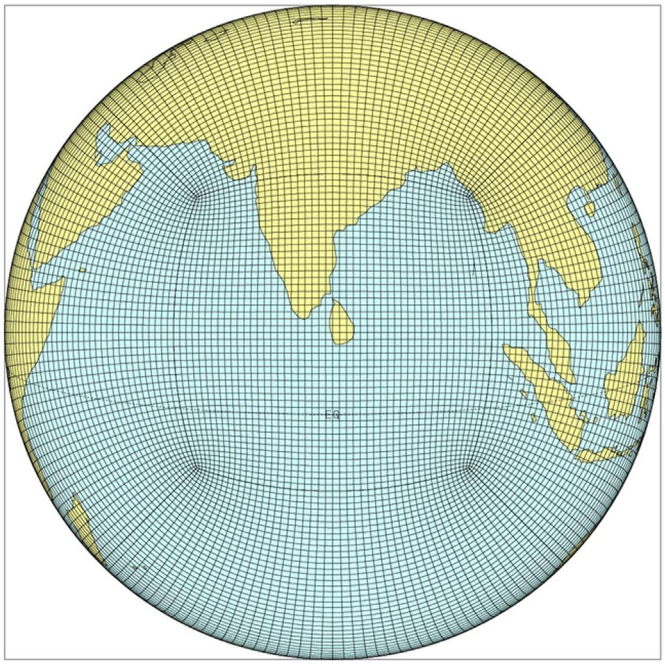

**Fig. 6.** The variable resolution grid used in the CCAM simulations undertaken for this study.

from 40 m to 35 km. The grid used in the CCAM application for this study resulted in a resolution of about 50 km over Sri Lanka. The model was forced with Sea Surface Temperatures taken from two of the IPCC Global Climate Models (ECHAM and GFDL) which performed well in the target area. CCAM output including winds, surface temperature, atmospheric pressure, radiation, ocean temperature etc. was thus obtained for the 1981–2000 (present) and 2081–2100 time slices at a temporal resolution of 6 h for the high end SRES A2 emissions scenario.

### 4.2. Regional/catchment scale coastal forcing models

#### 4.2.1. Riverflow

The CCAM output over Sri Lanka was used in a hydrologic model to derive riverflow estimates for the present (1981–2000) and future (2081–2100) (Mahanama and Zubair, 2011). The 6-hourly surface meteorological forcings used included shortwave radiation, longwave radiation, total precipitation, convective precipitation, surface pressure, air temperature, specific humidity, and wind for the two different periods. The hydrologic model used was the Catchment Land Surface Model (CLSM: Koster et al., 2000; Ducharne et al., 2000). CLSM is a macroscale hydrologic model that balances both surface water and energy at the Earth's land surface. CLSM considers irregularly shaped, topographically delineated, hydrologic catchments as the fundamental element on the land surface for computing land surface processes and has been successfully implemented in Sri Lanka using bias corrected reanalysis meteorological forcings (Mahanama et al., 2008). For this study, CLSM was forced in offline mode using CCAM downscaled surface meteorological forcings to generate riverflows into the 3 case study lagoons.

Available gridded precipitation data were used for bias correcting the downscaled ECHAM and GFDL precipitation hindcasts for the present time slice, which were then used in CLSM to simulate riverflows. Monthly riverflows from 22 gauge stations across Sri Lanka for the period 1979–1993 were used for validating CLSM for the hindcast period 1981–2000. As the ECHAM and GFDL projections for the 3 case study lagoons were very similar, only GFDL projections were used to construct the annual cycle of riverflows to use as future forcing in the Coastal impact model, *Delft3D*. Here *Delft3D* was used with a

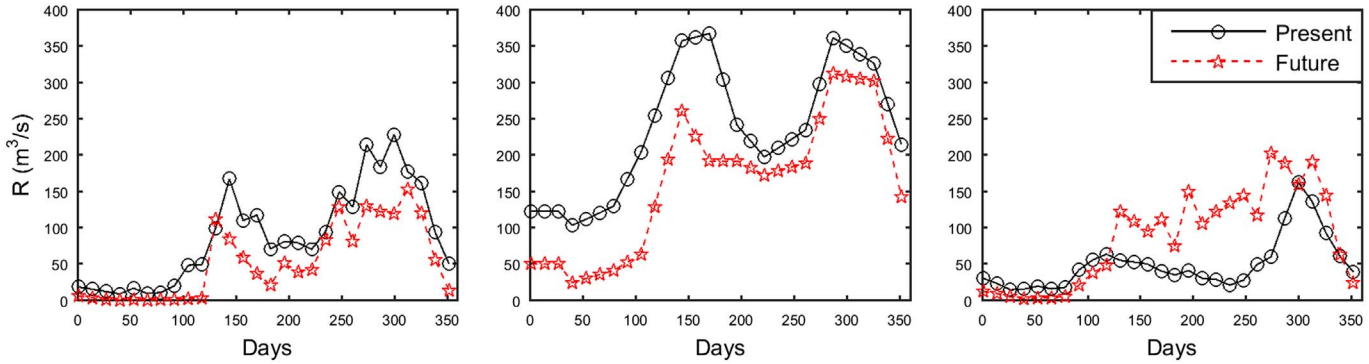


**Fig. 7.** Contemporary and year 2100 riverflow forcing time series for Negombo lagoon (left), Kalutara lagoon (middle), and Maha Oya river (right).

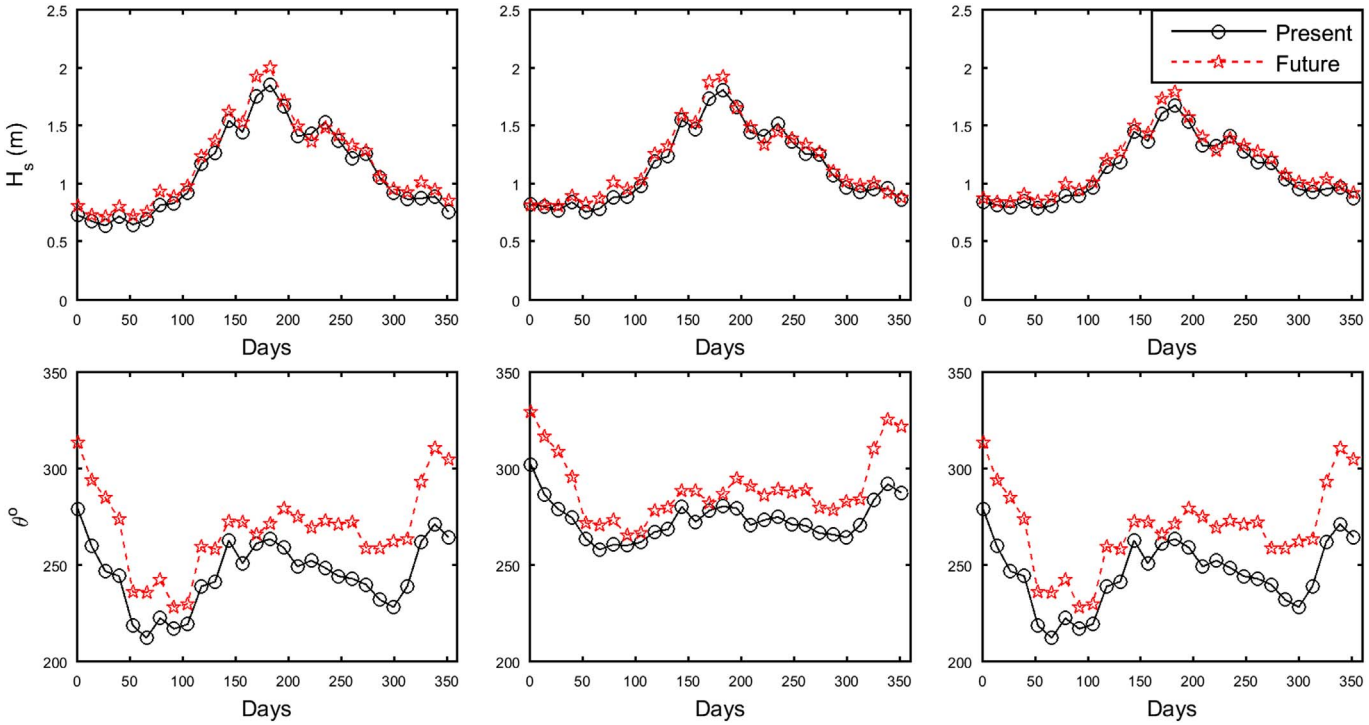


**Fig. 8.** Contemporary and year 2100 wave time series (at 20 m depth) for Negombo lagoon (left), Kalutara lagoon (middle), and Maha Oya river (right). Significant wave height ($H_s$) (top), mean wave direction ($\theta$) (bottom).

morphological acceleration factor (MORFAC, Roelvink, 2006) of 13 to ensure the representation of the spring-neap cycle in the CC impact assessments (see Section 5.1 below), and therefore, 13-day averaged riverflows were used to construct the annual riverflow time series (Fig. 7) to force the process based snap-shot model simulations described below in Section 5. In general, by 2100, riverflow is projected to decrease by about 41% and 32% at Negombo lagoon and Kalutara lagoon respectively, while an increase of about 72% is projected for Maha Oya river.

#### 4.2.2. Waves

CCAM winds were used to force two nested spectral wave models for 1981–2000 (hindcast) and 2081–2100 (future) time slices (Bamunawala, 2013). Due to the similarity between CCAM downscaled ECHAM and GFDL winds in the study area, only CCAM-GFDL winds were used in this analysis. For the generation of far field waves, WAVEWATCH III (Tolman, 2009) was used (Latitudes N22°–S7°; Longitudes E65°–E95°). SWAN (Booij et al., 1999) was used in the near field from about 50 m depth to the coastline extending from Galle to Puttalam along the SW coast (see Fig. 1 for locations). Modelled wave conditions for the hindcast period were compared against available deep water wave data off Colombo. The bias correction required to ensure a good model/data comparison was then determined and applied to the future projected wave conditions with the commonly adopted assumption that present-day biases between model and reality will remain the same in future (Charles et al., 2012; Wang et al., 2015). Bias corrected SWAN model output at 20 m depth offshore of the 3 case study sites were computed to use as boundary forcing in the process based snap-shot model simulations described in Section 5 below. As the process based model *Delft3D* was used with a MORFAC of 13 to ensure the representation of the spring-neap cycle in the CC impact assessments (see Section 5.1), 13-day averaged wave heights and directions were used to construct the annual time series of wave conditions for model forcing (Fig. 8).

### 4.3. Coastal impact modelling

The process based coastal area model *Delft3D* was used for all morphodynamic simulations undertaken in this study. For each of the 3 case study applications in this study, identical wave and flow domains which were large enough to avoid any boundary problems affecting the area of interest were created (Fig. 9). High resolution (~10 m × 10 m)

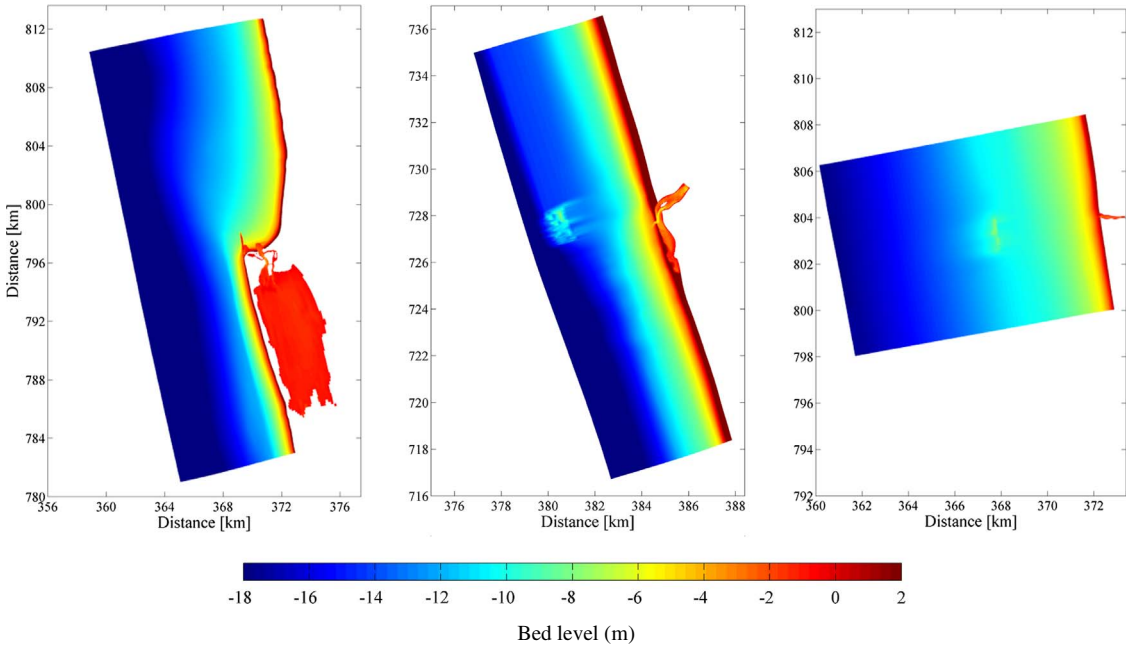


**Fig. 9.** Wave/flow domains used for Negombo (left), Kalutara (middle) and Maha Oya (right).

**Table 3**
Data used for hydrodynamic model validation at the case study sites.

| STI System | Data type | Data period |
|---|---|---|
| Negombo lagoon | Water level | 01–30 Oct 2002 |
| | Velocity | 02–03 Oct 2002 |
| Kalutara lagoon | Water level | 13–26 Feb 2013 |

grid cells were used in the (approximate) surf zone and inlet channel for all 3 study areas to ensure that key physical processes in the vicinity of the inlet entrance and channel were accurately resolved by the model. Good measured bathymetries were available for all 3 case study sites.

## 5. Results

### 5.1. Model validation

#### 5.1.1. Hydrodynamic validation

First the models were validated against measured water level and velocity data in the study areas. Water level and velocity measurements for Negombo lagoon were available from a previous study. Two pressure sensors were deployed in Kalutara lagoon and Maha Oya river to collect water level data for this study specifically. Unfortunately however, due to problems with data acquisition, water level data at Kalutara lagoon was only captured intermittently, while the sensor deployed at Maha Oya river was lost. Therefore, hydrodynamic model

**Fig. 10.** Measurement locations of model validation data in Negombo lagoon (left) and Kalutara lagoon (right). Filled white circles: water level observation points (Negombo - S1: ocean side, S3: inside lagoon; Kalutara - K1: inside lagoon). Filled white triangles: velocity observation points (Negombo - CM1: inlet, CM2: inside lagoon). Red dotted circles: inlet mouth position. (For interpretation of the references to color in this figure legend, the reader is referred to the web version of this article.)

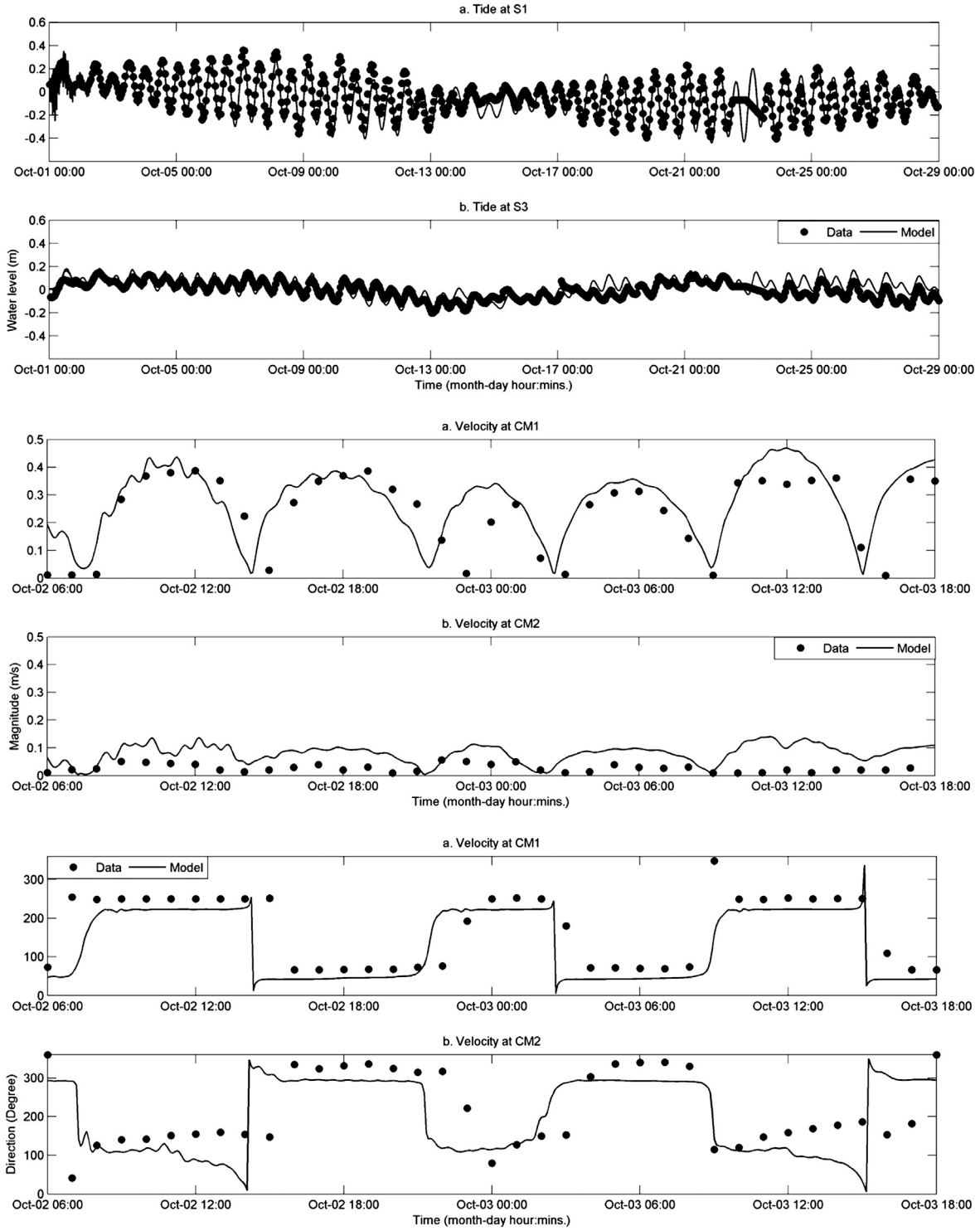


**Fig. 11.** Model/data comparisons of water levels and currents (magnitude and direction) at Negombo lagoon.

validation could only be undertaken for Negombo and Kalutara lagoons. The hydrodynamic validation simulations were undertaken with only tidal and riverflow forcing as wave effects are minimal within the 3 case study STIs. Tidal forcing constituted of astronomical tides composed of the 6 main tidal constituents in the area (M2, S2, N2, K2, K1, O1), and riverflow was introduced as a time series based on available measurements. Morphological updating was turned off in these short-term simulations.

The validation periods and data are shown in Table 3. The measurement locations are shown in Fig. 10. Based on the careful analysis of model results from over 50 sensitivity tests of the 3 case study sites and with the benefit of decades of in-house experience using *Delft3D* (and its predecessors) for coastal applications, a Chezy friction coefficient of 65 $m^{1/2}/s$, eddy viscosity of 1 $m^2/s$ and hydrodynamic time step of 6 s were adopted in all 3 hydrodynamic validation simulations. Model performance was assessed by computing the Root mean square error (RMSE) and the correlation coefficient ($R^2$) between corresponding modelled and measured water levels and velocities at the study sites. The model/data comparisons for Negombo and Kalutara lagoons (Figs. 11 and 12, and Table 4) are reasonably good, providing

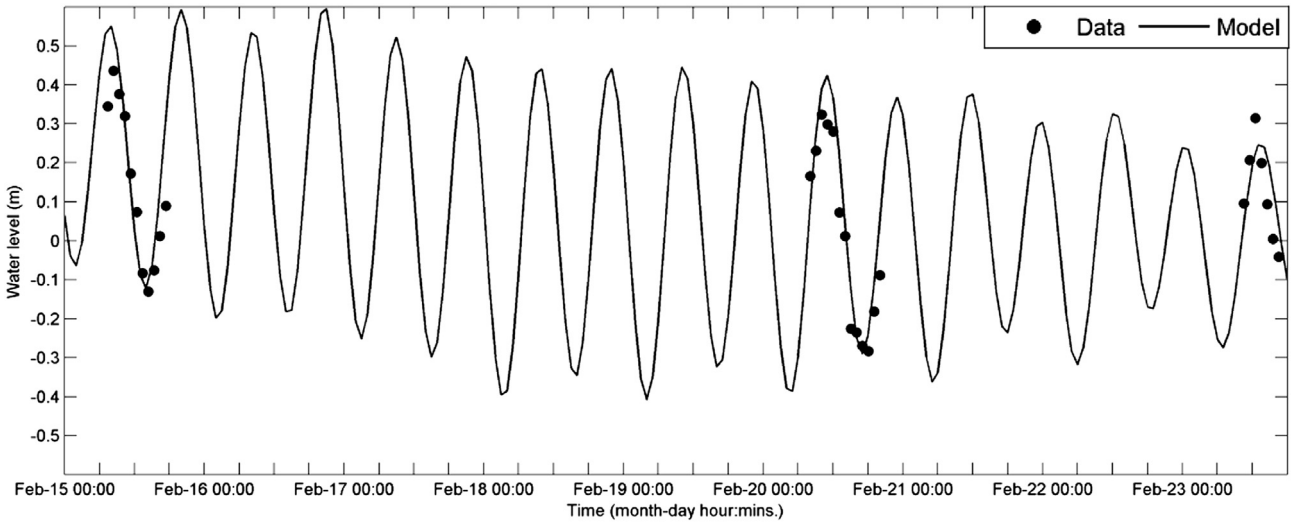


**Fig. 12.** Model/data comparison of water levels at Kalutara lagoon.

**Table 4**
Model/data comparison statistics for the hydrodynamic validation simulations.

| Negombo lagoon | | | | |
|---|---|---|---|---|
| Water level | S1 | | S3 | |
| | RMSE | $R^2$ | RMSE | $R^2$ |
| | 0.0325 | 0.9747 | 0.0312 | 0.8355 |

| Negombo lagoon | | | | |
|---|---|---|---|---|
| Current | CM1 | | CM2 | |
| | RMSE | $R^2$ | RMSE | $R^2$ |
| Current velocity | 0.1027 | 0.7319 | 0.0598 | 0.4397 |
| Current direction | 10.17 | 0.6890 | 14.59 | 0.5628 |

| Kalutara lagoon | | | | | | |
|---|---|---|---|---|---|---|
| | Feb 15 | | Feb 20 | | Feb 23 | |
| Water level | K1 | | K1 | | K1 | |
| | RMSE | $R^2$ | RMSE | $R^2$ | RMSE | $R^2$ |
| | 0.1155 | 0.8668 | 0.0776 | 0.9872 | 0.0538 | 0.8747 |

**Table 5**
Model parameter settings.

| Parameter | Adopted value |
|---|---|
| Hydrodynamic time step (s) | 6 |
| Hydrodynamic spin-up time (h) | 24 |
| Horizontal eddy viscosity ($m^2/s$) | 1 |
| Horizontal eddy diffusivity ($m^2/s$) | 0.1 |
| Chezy bottom friction coefficient ($m^{1/2}/s$) | 65 |
| Directional wave spreading (deg) | 10 (considering predominant swell conditions) |
| Sediment transport formula | van Rijn (1993) |
| Dry cell erosion factor | 0.5 |
| Wave-flow coupling interval (h) | 1 |
| MORFAC | 13 |
| Output interval for whole domain (h) | 1 |
| Output interval for pre-defined observation points and cross-sections (s) | 600 |

sufficient confidence in the models to proceed with the morphodynamic simulations.

### 5.1.2. Morphodynamic validation

For morphodynamic validation, a *Delft3D* simulation was undertaken with the above described contemporary forcing (i.e. 'Present simulation' - PS) at each system. In each case, astronomical tidal forcing was introduced at the offshore boundary using the tidal constituents presented by Wijeratne (2002). Riverflow/wave forcing was applied using the 13-day averaged time series shown in Figs. 7 and 8. A hydrodynamic spin up time of 24 h was used to ensure that model velocities were stable before sediment transport and morphological computations commenced. Model parameter values adopted, following Duong et al. (2017), are shown in Table 5.

A MORFAC of 13 was used in these simulations in order to capture two spring-neap cycles (29 days) of hydrodynamic forcing within a 1 year morphodynamic simulation. On top of the MORFAC = 13 simulations, a series of simulations were executed with MORFAC values of 1 and 5 to investigate the sensitivity of model predictions to the adopted MORFAC value (with appropriate changes in wave-flow coupling time and forcing time series). The MORFAC induced differences between model predictions in these sensitivity tests were very small, indicating that a MORFAC of 13 was appropriate for the simulations undertaken herein. Morphodynamic validation simulations for the permanently open Negombo lagoon (Type 1) and Kalutara lagoon (Type 2) were undertaken for one year, capturing the annual cycle of riverflow (high/low seasons) and wave conditions (monsoon/non-monsoon periods) while the simulation for the intermittently closing Maha Oya river (Type 3) was continued only until inlet closure occurred.

The main objective of the PS's is to gain confidence in the model's ability to correctly reproduce the general morphodynamic behaviour (e.g. close/open, and locationally stable/migrating) of the system under contemporary forcing. Therefore, as a first qualitative validation, the general behaviour of the systems as seen in available aerial/satellite images of the study areas was compared with that simulated by the models. In a more quantitative sense, modelled annual longshore sediment transport rates ($M$) and Bruun inlet stability criteria ($r = P/M$) were compared against reported values and observed inlet Type respectively. For these latter comparisons, quantitative information regarding the modelled annual longshore sediment transport rates ($M$), tidal prism ($P$) need to be extracted from model output. It should also be noted that the substantial riverflows in the 3 STIs investigated here enhance the ebb tidal prism (due to the tide effect only), which is one of the two phenomena that govern inlet stability. For convenience,

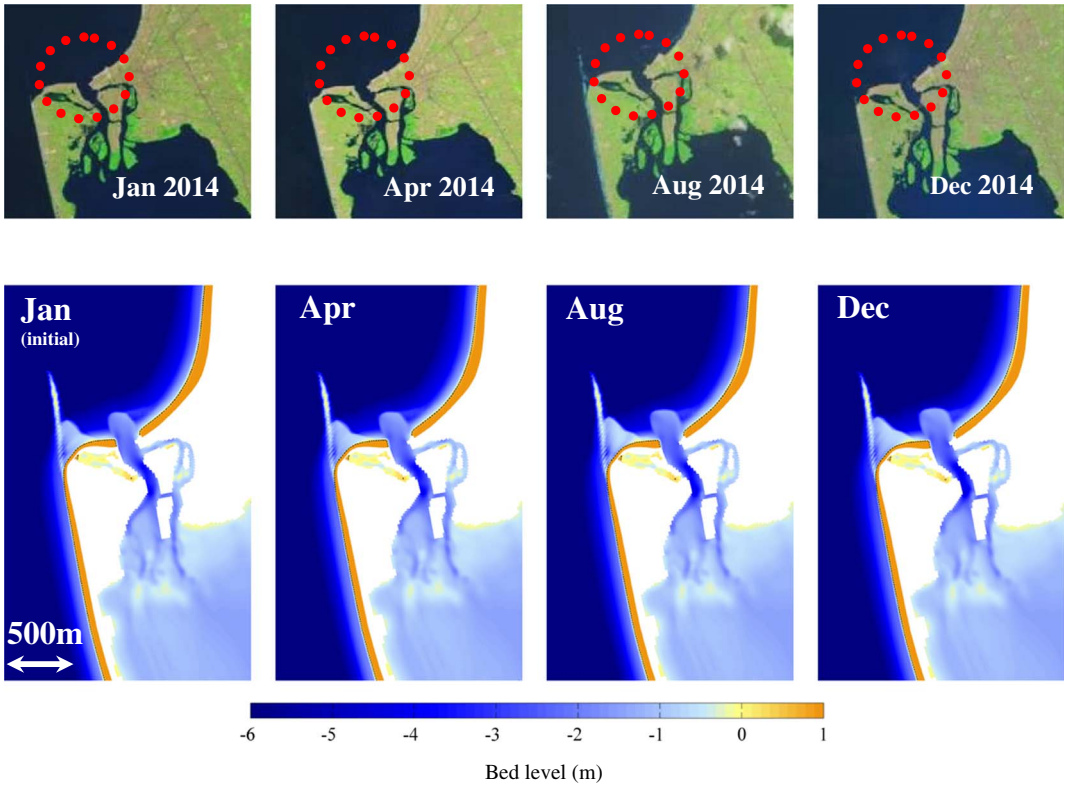


**Fig. 13.** Satellite images (top (source: *Landsat*)) and validation model results (bottom) of the annual bed level evolution of Negombo lagoon, showing the observed and modelled locationally and cross-sectionally stable inlet behaviour. In agreement with observations, the model results also do not indicate any significant morphological changes occurring within the annual forcing cycle. The red dotted circles in the satellite images indicate inlet location. The black line in the model results indicates the initial shoreline position. (For interpretation of the references to color in this figure legend, the reader is referred to the web version of this article.)

therefore, the flow volume through the inlet during ebb due to the combined effect of tides and riverflow is referred to hereon simply as tidal prism ($P$). Summary descriptions of the methods used to extract $P$ and $M$ from the model output are provided below.

To calculate $M$, the ambient annual longshore sediment transport (LST) volume needs to be computed. The ambient LST rate computed by the model is affected by the tidal inlet as well as the lateral model boundaries. This quantity therefore needs to be assessed sufficiently updrift of the inlet as well as sufficiently far from the updrift model boundary. Up to 10 cross-sections were pre-defined either side of the inlet (ensuring that the cross-sections spanned the full surf zone at all times) to determine the optimal alongshore location of the cross-shore section over which $M$ should be calculated. The optimal cross-shore section for ambient LST estimates was identified via a careful comparison of the modelled LST rates across all the pre-defined cross-shore sections. The annual ambient LST across the optimal cross-shore section ($M$) was then computed from the model output.

To compute $P$, cross-sections were pre-defined at every grid line (~10 m spacing) across the inlet channel and discharges were extracted and stored every 10 min (user defined output interval). $P$ was then estimated at each cross-section by calculating the difference between consecutive cumulative discharge peaks and troughs. Cumulative discharge is calculated by the model at every hydrodynamic time step (in this case, 6 s) and output at the pre-defined output interval (10 min). The tidal prism thus calculated did not vary along the inlet and therefore the $P$ calculated at the middle of the inlet channel was used in subsequent calculations.

The $M$ and $P$ values calculated as described above were combined to compute the Bruun criterion for inlet stability $r = P/M$. This produced a time series of $r$ which was time averaged to derive the annual representative $r$ indicating the general stability condition of the inlet.

Modelled bed level changes and satellite images for the 3 systems are shown in Figs. 13–15. Modelled and measured (reported) annual LST (or $M$) in the vicinity of the 3 inlets, the computed $r$ values, associated Bruun inlet stability classification and inlet Type following Table 2 are shown in Table 6.

Satellite images of Negombo lagoon show the locationally and cross-sectionally highly stable nature of this inlet (Fig. 13, top) which the model reproduces correctly (Fig. 13, bottom). The modelled annual longshore sediment transport in the vicinity of the inlet is small (42,000 $m^3$) in agreement with reported values (Table 6). The model derived Bruun criterion ($r$) value is 221 ($> 150$), which also indicates a very stable inlet following Table 2.

The Kalutara lagoon inlet has historically migrated about 2 km southward in 3–4 years, with an annual migration of ~500 m (Fig. 14a, top). When the migrating inlet reaches the southern end of the barrier between the lagoon and the ocean (beyond which it is physically impossible for the inlet to migrate), a new, more hydraulically efficient inlet has traditionally been naturally or artificially created at the northern end of the lagoon, starting off a new migration cycle (Fig. 14a, top). The locationally unstable and cross-sectionally stable inlet behaviour seen in the satellite images is correctly reproduced by the validation simulation (Fig. 14a, bottom). The modelled annual longshore sediment transport of 562,000 $m^3$ to the south and the migration rate of about 600 m/yr to the south (Fig. 14b), are both in agreement with reported values (Table 6 and Perera, 1993). The model derived Bruun criterion ($r$) value is 11 ($< 20$), which indicates an unstable inlet following Table 2. This $r$ value of 11 for the alongshore migrating but permanently open Kalutara inlet implies that the Bruun criteria definition of an 'unstable inlet' when $r < 20$ applies to locational stability and not to cross-sectional stability. This is consistent with the results of the data poor approach for Type 2 STIs presented in Duong et al. (2017).

The validation simulation for Maha Oya inlet reproduces the locationally stable and cross-sectionally unstable inlet behaviour seen in satellite images of this system (Fig. 15a). The modelled inlet closure

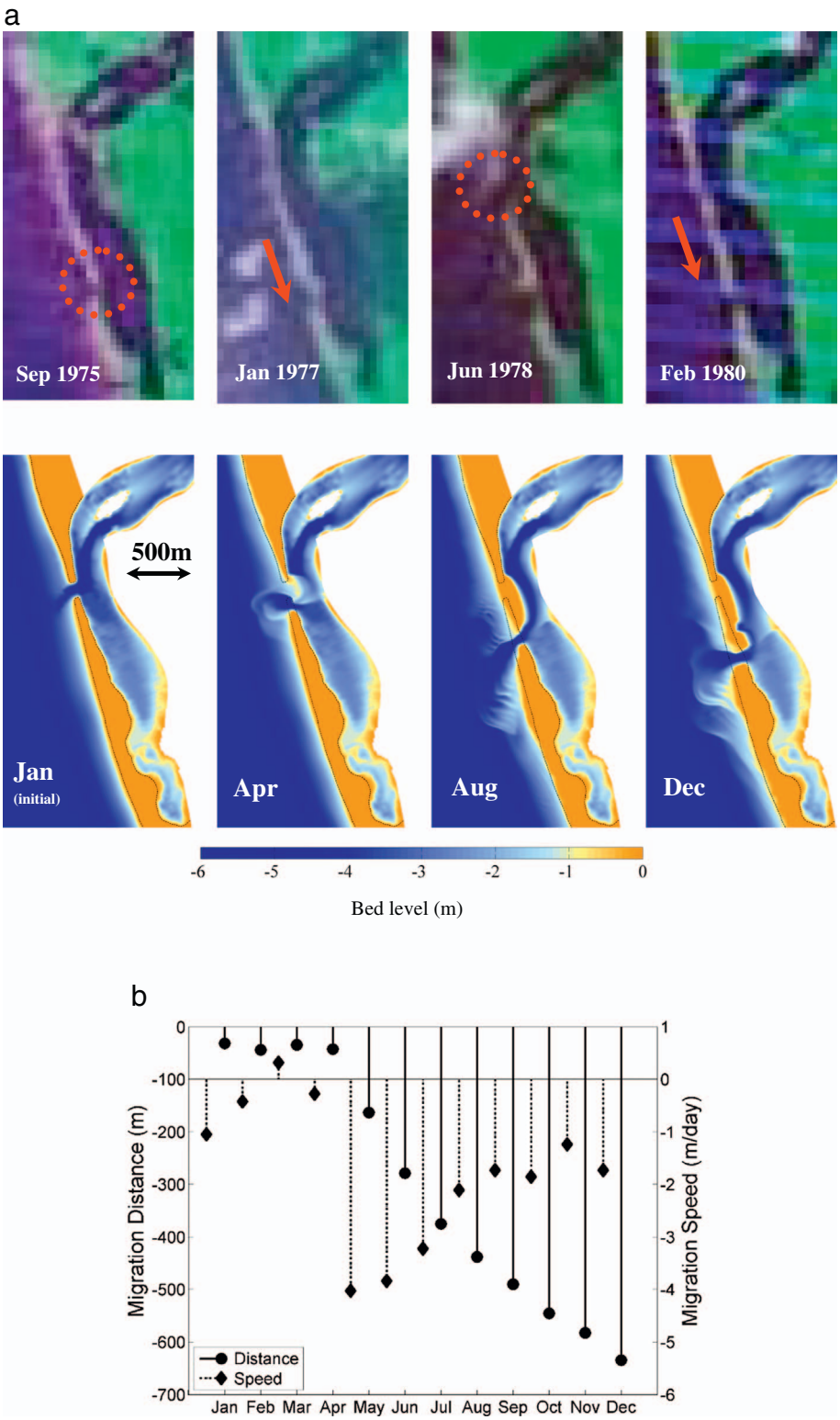


**Fig. 14.** (a) Satellite images (top (source: *Landsat*)) and validation model results (bottom) of the annual bed level evolution of the Kalutara lagoon inlet, showing the observed and modelled locationally unstable and cross-sectionally stable inlet behaviour with the model correctly reproducing the observed southward migration of about 500 m/yr (see also Fig. 14b). The red dotted circles in the satellite images indicate inlet location and the red arrows indicate migration direction. The black line in the model results indicates the initial shoreline position.
(b) Modelled inlet migration distance and speed (monthly averaged) through the 1 year validation simulation of Kalutara lagoon inlet showing that the model correctly reproduces observed southward (negative = southward) migration rate of ~500 m/yr and higher migration speeds during the SW monsoon. (For interpretation of the references to color in this figure legend, the reader is referred to the web version of this article.)

occurs 45 days into the simulation. The time evolution of the modelled inlet cross-sectional area shown in Fig. 15b further illustrates the complete closure of the inlet after 45 days. The modelled annual longshore sediment transport of 450,000 $m^3$ to the North is in agreement with reported values (Table 6). The Bruun criterion ($r$) value calculated using model derived $P$ and $M$ values for Maha Oya inlet is 1 ($< 20$), which correctly indicates an unstable inlet following Table 2. However, consistent with the results of the data poor approach for Type 3 STIs presented in Duong et al. (2017), this very low $r$ value of 1 implies that an $r$ value much lower than Bruun's threshold for unstable conditions ($r = 20$) may be necessary for an inlet to be cross-sectionally unstable.

In summary, the above results show that the model is able to reproduce contemporary observed behaviour of the 3 case study STIs, providing sufficient confidence to proceed with CC impact assessments.

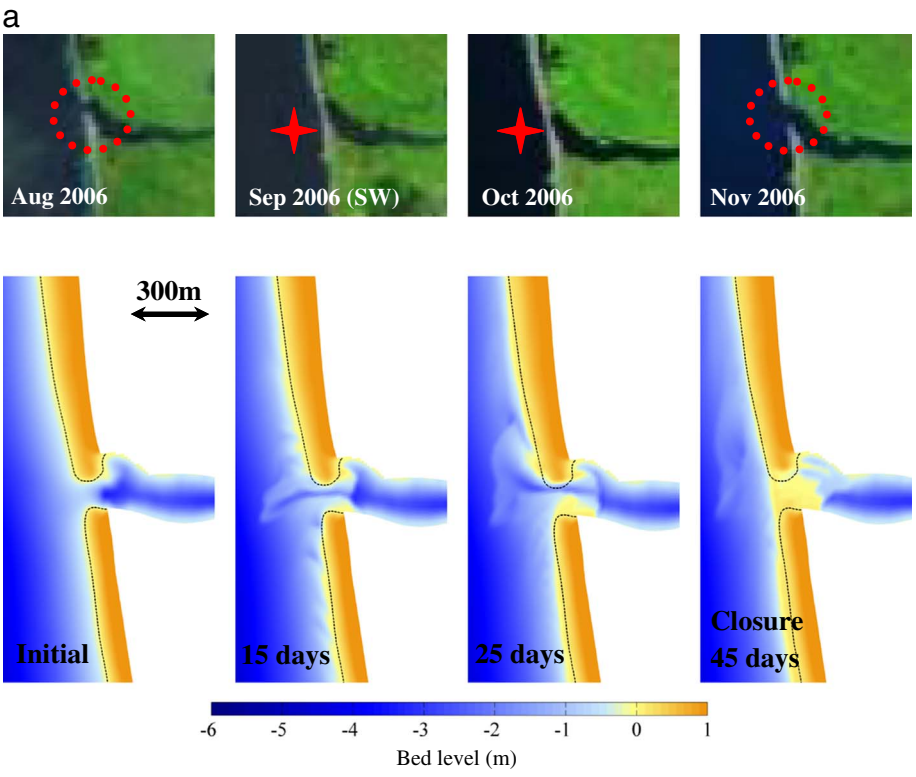


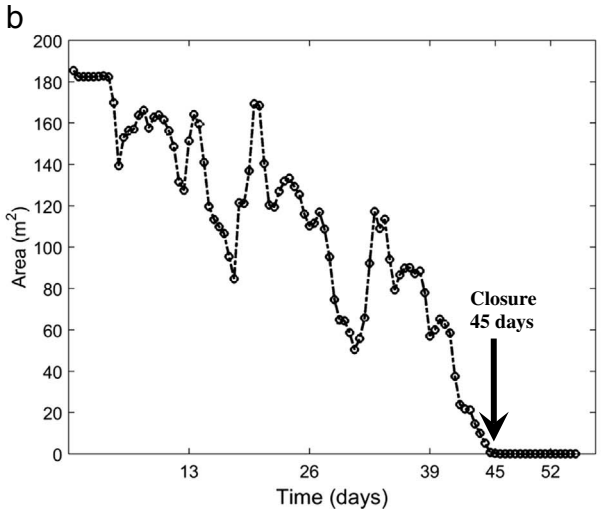


**Fig. 15.** (a) Satellite images (top (source: *Landsat*)) and validation model results (bottom) showing the bed level evolution of the Maha Oya river inlet, showing the observed and modelled locationally stable and cross-sectionally unstable inlet behaviour. The red dotted circles in the satellite images indicate inlet location when the inlet is open. The red asterisks indicate the occasions when the inlet is closed. Black line in model results shows initial coastline.
(b) Time evolution of inlet cross-sectional area in the validation simulation of Maha Oya river showing that the model correctly reproduces observed inlet closure. (For interpretation of the references to color in this figure legend, the reader is referred to the web version of this article.)

**Table 6**
Modelled and measured (reported) annual LST ($M$) in the vicinity of the 3 case study inlets (S and N indicate southward and northward transports respectively), the model derived Bruun criterion $r$, the corresponding Bruun stability classification, and inlet Type following Table 2.

| STI system | Reported $M$ ($m^3$/yr) | Modelled $M$ ($m^3$/yr) | $r = P/M$ | Bruun stability classification | Inlet Type |
|---|---|---|---|---|---|
| Negombo lagoon | 20,000 S | 42,000 S | 221 | Good | 1 |
| Kalutara lagoon | 500,000 S | 562,000 S | 11 | Unstable | 2 |
| Maha Oya river | 500,000 N | 450,000 N | 1 | Unstable | 3 |

### 5.2. CC impact assessment

For each STI system, the validated model was then implemented via snap-shot simulations to investigate future CC impacts on the system. These simulations were also undertaken for the same duration as the validation simulations, or, in the case of Maha Oya river, until inlet closure occurred. For each STI, CC modified riverflow and wave forcing were implemented using the projected forcing shown in Figs. 7 and 8. A worst case SLR of 1 m (by 2100 relative to the present) was applied at all 3 systems. The tidal forcing of all CC impact simulations were the same as that used in the corresponding validation simulations.

Due to the spatially non-uniform bathymetries of the systems, SLR driven basin infilling was implemented differently compared to the simple spatially uniform raising of the lagoon/inlet bed level method used in the flat-bed schematized models employed in Duong et al.

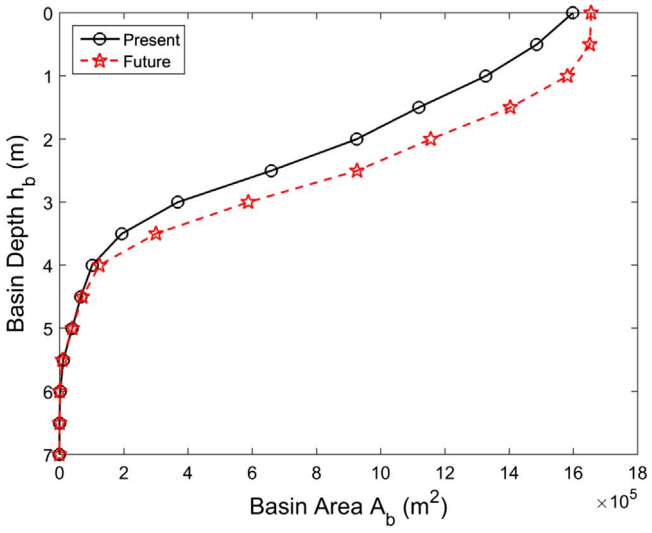


**Fig. 16.** Present and future (year 2100) basin hypsometry curves indicative of the implemented bed level changes in Kalutara lagoon to represent SLR driven basin infilling.

(2017). Here, the bed levels of the initial measured bathymetry were changed to accommodate the basin infill volume (calculated as total infill volume = 0.5 x SLR x $A_b$, where $A_b$ = surface area of lagoon, or basin; Ranasinghe et al., 2013) such that the shapes of the present and future basin hypsometry curves were more or less the same. Basin hypsometry is the relationship between the basin depth ($h_b$) (measured from surface to the bottom, elevation = 0 at surface) and the basin area ($A_b$) (measured from bottom to surface, with area = 0 at the bottom) (Boon and Byrne, 1981). Essentially, the shape of the basin hypsometry curve reflects the channel-shoal structure of a basin, which can be reasonably assumed to remain more or less unchanged as long as natural and/or human induced disturbances to the morphological equilibrium of the system are not too large. For example, Wang et al. (2002) have shown that the hypsometry of the Western Scheldt estuary (The Netherlands) follow the same relatively simple algebraic relation through time despite the morphological developments driven by relative SLR as well as human interferences.

To estimate the bed level changes required to represent basin infilling in this way, first it is assumed that at all grid points:

$$h_{b,f} = (h_{b,p} + SLR) - \Delta h \quad (1)$$

where $\Delta h$ is assumed to follow the general depth transfer function given by,

$$\Delta h = a'(h_{b,p} + SLR) \quad (2)$$

where $a'$ is a coefficient, of which the optimal value is found via iteration. Subscripts '*p*' and '*f*' represent *present* and *future* respectively.

As an example, the year 2100 basin hypsometry curve calculated for Kalutara lagoon using the above approach is shown in Fig. 16, together with the contemporary hypsometry curve.

### 5.2.1. *Negombo lagoon*

The modelled future morphological changes over one year for the Type 1 Negombo lagoon are shown in Fig. 17. For easy comparison, the validation simulation results for this STI shown in Fig. 13 are also reproduced in Fig. 17 (top panels). Model results show that this STI will remain a locationally and cross-sectionally stable inlet by 2100. The *r* value however decreases to 75, from its present value of 221. This is due to the future increase in southward *M* resulting from the CC driven clockwise rotation of waves (see Fig. 8). According to Bruun's inlet stability classification (Table 2), this implies that the level of stability of the inlet will decrease from 'good' to 'fair to poor'.

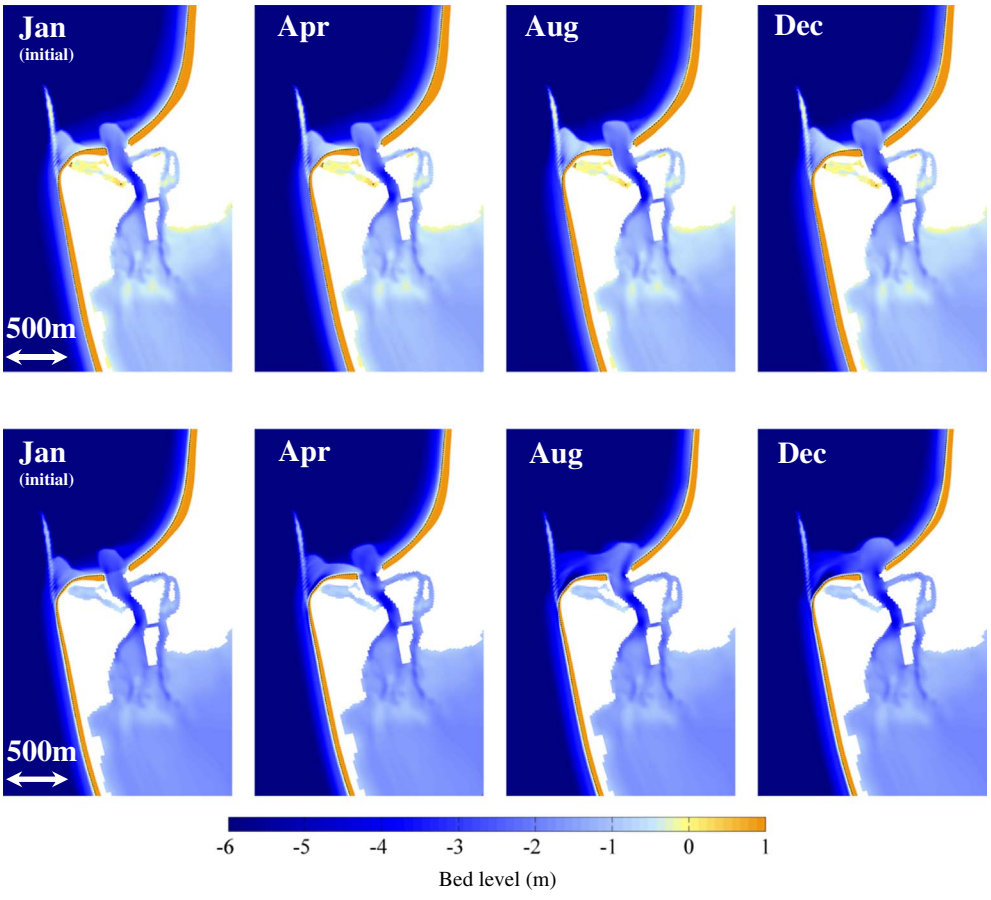


**Fig. 17.** Modelled morphological changes for Negombo lagoon over a one year period; under contemporary forcing conditions (top) and CC modified year 2100 forcing conditions (bottom). Neither simulation indicates any significant morphological changes occurring within the annual forcing cycle. The black line indicates the initial shoreline position. (For interpretation of the references to color in this figure legend, the reader is referred to the web version of this article.)

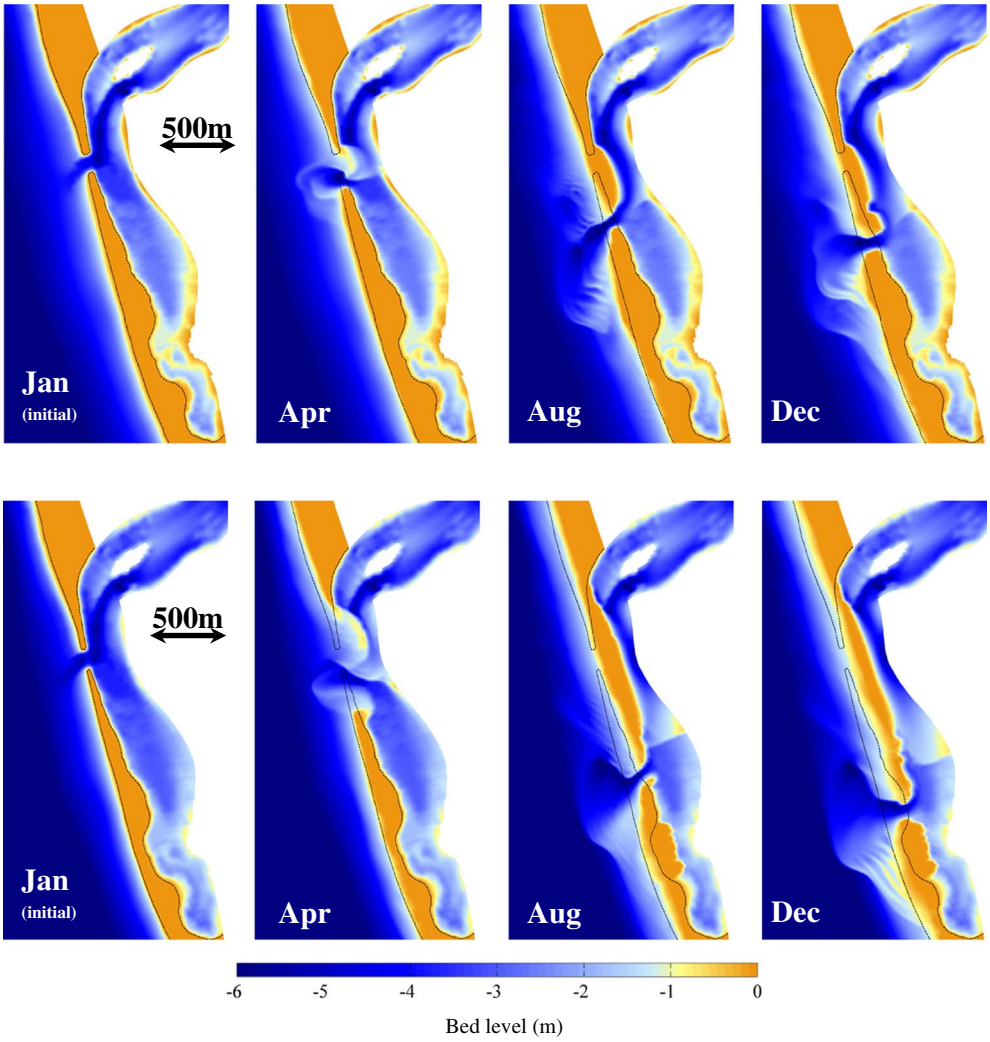


**Fig. 18.** Modelled morphological changes for Kalutara lagoon over a one year period; under contemporary forcing conditions (top) and CC modified year 2100 forcing conditions (bottom). The black line indicates the initial shoreline position. (For interpretation of the references to color in this figure legend, the reader is referred to the web version of this article.)

*5.2.2. Kalutara lagoon*

The modelled future morphological changes over one year for the Type 2 Kalutara lagoon are shown in Fig. 18, together with corresponding validation simulation results. Model results show that Kalutara lagoon will remain a permanently open, alongshore migrating Type 2 STI by year 2100. However the migration distance doubles to ~1200 m, while the *r* value decreases to 6 from its present value of 11. These changes can be directly attributed to the future increase in southward *M* due the CC driven clockwise rotation of waves (see Fig. 8).

*5.2.3. Maha Oya river*

The modelled future morphological changes for the Type 3 Maha Oya river are shown in Fig. 19, together with corresponding validation simulation results. Model results show that this STI will remain an intermittently open, locationally stable Type 3 STI by year 2100. However the time until inlet closure increases by about 75% from its modelled present value of 45 days to 78 days, while the *r* value slightly increases to 5 from its present value of 1. These changes in system behaviour are due to the combined effect of the future increase in annual riverflow (see Fig. 7) and the smaller northward *M* resulting from the CC driven clockwise rotation of waves (see Fig. 8).

Comparison of future projections of inlet Type and changes in main behavioural characteristics obtained from the data poor and data rich approaches (Table 7) shows very good agreement for each of the 3 STIs. This provides a type of validation for the low-cost data poor approach, indicating that the approach may be used with confidence even in data rich environments to obtain qualitative insights at low cost. It is however, noteworthy that the time to closure of the Type 3 system shows a significant difference (~100% difference) between the two approaches. Furthermore, the data rich approach also provides detailed and site specific information on where future erosion/accretion may be expected in and around STIs, which is essential for the development of informed and effective local scale CC adaptation strategies in STI environs.

*5.3. Relative contributions of CC driven variations in system forcing to inlet stability*

For each case study site, four additional simulations where CC forcing was sequentially removed (Simulations R2-R5; R1 being the above discussed 'all inclusive' CC impact simulation) were undertaken to investigate the relative contribution of the different CC forcings to future inlet stability. The CC forcings implemented in each simulation are shown in Table 8. Note that when CC modified future forcing is not used in a certain simulation, the present day values are still used for that forcing type in the year 2100 snap-shot simulation (i.e. representing a scenario where there is no CC driven variation in the future forcing). For example, in R2, the present day riverflow shown in Fig. 7 was used (i.e. no CC driven variation in riverflow is imposed in R2). Also, basin infilling was not included in simulations that excluded SLR (i.e. R5). When SLR is implemented (Simulations R1-R4), it was specified as 1 m. This set of simulations can be used to determine the effect

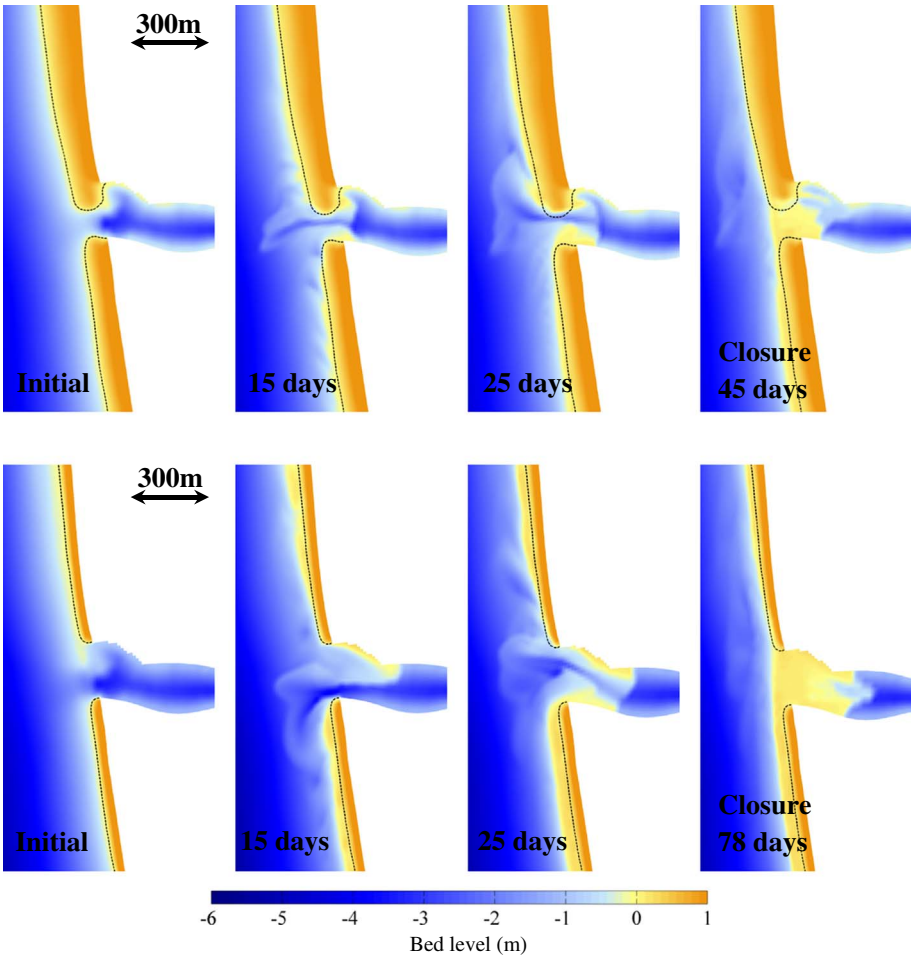


**Fig. 19.** Modelled morphological changes for Maha Oya river until inlet closure; under contemporary forcing conditions (top) and CC modified year 2100 forcing conditions (bottom). The black line indicates the initial shoreline position. (For interpretation of the references to color in this figure legend, the reader is referred to the web version of this article.)

**Table 7**
Comparison of year 2100 projections obtained from the data poor and data rich approaches for the 3 case study sites.

| STI system | Present inlet Type | Changes in system forcing by 2100 | Projected inlet Type and behaviour by 2100 | |
|---|---|---|---|---|
| | | | Data poor approach | Data rich approach |
| Negombo lagoon | Type 1 | *SLR*,*M* +,*P* − | Type 1 | Type 1 |
| Kalutara lagoon | Type 2 | *SLR*,*M* +,*P* − | Type 2, ~100% more migration | Type 2, ~100% more migration |
| Maha Oya river | Type 3 | *SLR*,*M* −,*P* + | Type 3, open ~150% longer | Type 3, open ~75% longer |

Note: The comparable data poor approach simulations from Duong et al. (2017) are: C11 for Negombo lagoon, C11 for Kalutara lagoon and C14 for Maha Oya river.

**Table 8**
Forcing conditions implemented in the different CC forcing simulations. Subscript '*f*' indicates *future* conditions.

| | SLR | $H_{Sf}$,$\theta_f$ | $R_f$ |
|---|---|---|---|
| R1 | x | x | x |
| R2 | x | x | |
| R3 | x | | x |
| R4 | x | | |
| R5 | | x | x |

**Table 9**
Model predicted year 2100 STI types and inlet behavioural characteristics in response to different CC forcings.

| Simulation | Negombo lagoon | | Kalutara lagoon | | | Maha Oya river | | |
|---|---|---|---|---|---|---|---|---|
| | *r* | Type | *r* | Migration distance (m) | Type | *r* | Time till closure (days) | Type |
| R1 | 75 | Type 1 | 6 | 1210 | Type 2 | 5 | 78 | Type 3 |
| R2 | 82 | Type 1 | 7 | 1183 | Type 2 | 4 | 72 | Type 3 |
| R3 | 128 | Type 1 | 7 | 914 | Type 2 | 1 | 65 | Type 3 |
| R4 | 142 | Type 1 | 9 | 851 | Type 2 | 1 | 65 | Type 3 |
| R5 | 83 | Type 1 | 6 | 1067 | Type 2 | 4 | 72 | Type 3 |

of CC driven changes in each of the system forcings on future STI behaviour. For example, the difference between R2 and R1 would be indicative of the isolated effect CC driven changes in annual riverflow would have on STI behaviour, while differences between R5 and R1 would provide insights on the effect of SLR.

The main results from this set of simulations are summarised in Table 9. The results of the validation simulation (R1) are also shown for easy comparison.

The results in Table 9 indicate that the presence or absence of CC driven changes in any *one* system forcing is not capable of changing the *Type* of any of the 3 case study STIs.

For Negombo lagoon, the results indicate that CC driven changes in wave conditions (in this case with an associated increase in *M*) have the largest impact on inlet stability, accounting for almost 70% of overall

CC modified $r$ value of 75 (by comparing $r$ for R1, R3 and R4). Comparison of results for R1, R2 and R5 indicates that CC driven variations in riverflow and SLR both appear to have smaller but similar contributions to the overall CC effect on inlet stability (~10% contribution).

For Kalutara lagoon, the variations among $r$ values computed for the 5 simulations are insignificant and stay within the $5 < r < 10$ range. Nevertheless, the variations in migration distance indicate that the phenomenon which contributes most to the 1210 m of migration due to combined CC forcing (R1) is CC driven variations in wave conditions (R3, 25% contribution to the overall migration distance).

At Maha Oya, while both the $r$ value and time to closure for all simulations vary very little, the biggest drops in both diagnostics are attributable to CC driven variations in wave conditions (by comparing R1, R3 and R4).

The above results show that, at all 3 case study sites, the CC effect that dominates future changes in STI behaviour is CC driven variations in wave conditions, and not SLR as is commonly thought. This is consistent with the conclusions derived from the application of the 'data poor' modelling approach by Duong et al. (2017).

## 6. Conclusions

A snap-shot simulation approach using the process based coastal area morphodynamic model *Delft3D* has been applied to assess CC impacts on the stability of Small Tidal Inlets (STIs). The modelling approach was applied to three case study sites representing the main types of STIs: locationally and cross-sectionally stable inlets (Type 1, Negombo lagoon, Sri Lanka - permanently open, fixed in location); cross-sectionally stable, locationally unstable inlets (Type 2, Kalutara lagoon, Sri Lanka - permanently open, alongshore migrating); and locationally stable, cross-sectionally unstable inlets (Type 3, Maha Oya river, Sri Lanka - intermittently open, fixed in location). Future CC modified wave and riverflow conditions were derived from a regional scale application of spectral wave models (WaveWatch III and SWAN) and catchment scale applications of a hydrologic model (CLSM) respectively, both of which were forced with IPCC GCM output dynamically downscaled to ~50 km resolution over the study area with the stretched grid Conformal Cubic Atmospheric Model CCAM.

The coastal impact model used in this study, *Delft3D*, was successfully validated for contemporary conditions using short-term hydrodynamic measurements and reproduced the general morphological behaviour observed in satellite images of the study sites. Subsequent CC impact simulations undertaken with the validated models forced by projected SLR, waves and riverflows for the end of the 21st century indicate the following:

- None of the 3 case study STIs will change Type by the year 2100.
- By the end of the 21st century, the level of stability of the Negombo lagoon, as indicated by the Bruun criterion $r$, will decrease from 'Good' to 'Fair to poor'. The level of (locational) stability of the Kalutara lagoon, as indicated by the doubling of the annual migration distance, will also decrease. At Maha Oya river, the time till inlet closure will increase by about 75%, indicating an increase in the level of stability of this inlet.
- CC driven variations in wave conditions, and resulting changes in the annual longshore sediment transport, is the main contributor to the overall CC effect on the stability of all 3 STIs. SLR and CC driven variations in riverflows play only a rather secondary role.

Results obtained herein by applying the 'data rich' approach to the 3 case study sites are in good agreement with those obtained for similar trends in CC driven variations in forcing using the 'data poor' approach presented in the companion article (Duong et al., 2017), providing more confidence in the robustness of the low-cost 'data poor' approach. However, the 'data rich' approach provides more detailed and reliable site specific information on likely future morphological changes in and around STIs which is essential for effective on-the-ground coastal zone management/planning. Therefore, as a basic guideline, it is suggested that the 'data poor' approach be applied when only qualitative insights into how CC might affect the stability of STIs are required, and the 'data rich' approach be applied when quantitative information is required for the development of informed and effective site specific CC adaptation strategies, especially at Type 2 and Type 3 STIs at which significant future behavioural changes could occur.

## Acknowledgments

TMD was supported by the UNESCO-IHE and DGIS (Dutch foreign ministry) cooperation program UPARF. RR is supported by the AXA Research fund and the Deltares Harbour, Coastal and Offshore engineering Research Programme '*Bouwen aan de Kust*'. The international Association of Dredging companies (IADC) and IHE Delft are gratefully acknowledged for providing the funding required for open access publication of this article.

## References

Bamunawala, R.M.J., 2013. Impact of Climate Change on the Wave Climate of Sri Lanka (MPhil Thesis). University of Moratuwa, Sri Lanka (55p).
Booij, N., Ris, R.C., Holthuijsen, L.H., 1999. A third generation wave model for coastal regions. Part 1: model description and validation. J. Geophys. Res. 104 (C4), 7649–7666.
Boon, J.D., Byrne, R.J., 1981. On basin hypsometry and the morphodynamic response of coastal inlet systems. Mar. Geol. 40, 27–48.
Bruun, P., 1978. Stability of tidal inlets – theory and engineering. Developments in Geotechnical Engineering. Elsevier Scientific, Amsterdam (510p).
Bruun, P., Gerritsen, F., 1960. Stability of Coastal Inlets. North-Holland Publishing Co., Amsterdam (123pp).
Chandramohan, P., Nayak, B.U., 1990. Longshore - transport model for South Indian and Sri Lankan coasts. J. Waterw. Port Coast. Ocean Eng. 116, 408–424.
Charles, E., Idier, D., Delecluse, P., Deque, M., Le Cozannet, G., 2012. Climate change impact on waves in the Bay of Biscay. Ocean Dyn. 62, 831–848.
Dodet, G., Bertin, X., Bruneau, N., Fortunato, A.B., Nahon, A., Roland, A., 2013. Wave-current interactions in a wave-dominated tidal inlet. J. Geophys. Res. Oceans 118, 1587–1605.
Ducharne, A., Koster, R.D., Suarez, M.J., Stieglitz, M., Kumar, P., 2000. A catchment-based approach to modeling land surface processes in a GCM, part 2, parameter estimation and model demonstration. J. Geophys. Res. 105, 24823–24838.
Duong, T.M., Ranasinghe, R., Walstra, D.J.R., Roelvink, D., 2016. Assessing climate change impacts on the stability of small tidal inlet systems: why and how? Earth-Sci. Rev. 154, 369–380.
Duong, T.M., Ranasinghe, R., Luijendijk, A., Waltsra, D.J.R., Roelvink, D., 2017. Assessing climate change impacts on the stability of small tidal inlets - part 1: data poor environments. Mar. Geol. 390, 331–346.
GTZ, 1994. Longshore Sediment Transport Study for the South West Coast of Sri Lanka. Project Report. (25p).
Hemer, M., Fan, Y., Mori, N., Semedo, A., Wang, X.L., 2013. Projected changes in wave climate from a multi-model ensemble. Nat. Clim. Chang. 3, 471–476.
IPCC, 2013. Summary for policymakers. In: Stocker, T.F., Qin, D., Plattner, G.-K., Tignor, M., Allen, S.K., Boschung, J., Nauels, A., Xia, Y., Bex, V., Midgley, P.M. (Eds.), Climate Change 2013: The Physical Science Basis. Contribution of Working Group I to the Fifth Assessment Report of the Intergovernmental Panel on Climate Change. Cambridge University Press, Cambridge, United Kingdom and New York, NY, USA.
Koster, R.D., Suarez, M.J., Ducharne, A., Stieglitz, M., Kumar, P., 2000. A catchment-based approach to modeling land surface processes in a GCM, part 1, model structure. J. Geophys. Res. 105, 24809–24822.
Lesser, G., Roelvink, J.A., Van Kester, J.A.T.M., Stelling, G.S., 2004. Development and validation of a three-dimensional morphological model. Coast. Eng. 51, 883–915.
Mahanama, S.P.P., Zubair, L., 2011. Production of Streamflow Estimates for the Climate Change Impacts on Seasonally and Intermittently Open Tidal Inlets (CC-SIOTI) Project. FECT Technical Report 2011-01: Foundation for Environment, Climate and Technology, Digana Village, October, 2011. (20p).
Mahanama, S.P.P., Koster, R.D., Reichle, R.H., Zubair, L., 2008. The role of soil moisture initialization in sub-seasonal and seasonal streamflow prediction - a case study in Sri Lanka. Adv. Water Resour. 31, 1333–1343.
McGregor, J., Dix, M., 2008. An updated description of the conformal cubic atmospheric model. In: Hamilton, K., Ohfuchi, W. (Eds.), High Resolution Simulation of the Atmosphere and Ocean. Springer, pp. 51–76.
Nienhuis, J.H., Ashton, A.D., Nardin, W., Fagherazzi, S., Giosan, L., 2016. Alongshore sediment bypassing as a control on river mouth morphodynamics. J. Geophys. Res. Earth 121, 664–683.
Perera, J.A.S.C., 1993. Stabilization of the Kaluganga river mouth in Sri Lanka (M.Sc Thesis Report) In: International Institute for Infrastructural Hydraulic and Environmental Engineering, Delft, The Netherlands, (97p).

Ranasinghe, R., 2016. Assessing climate change impacts on open sandy coasts: a review. Earth-Sci. Rev. 160, 320–332.
Ranasinghe, R., Swinkels, C., Luijendijk, A., Roelvink, D., Bosboom, J., Stive, M., Walstra, D., 2011. Morphodynamic upscaling with the MORFAC approach: dependencies and sensitivities. Coast. Eng. 58, 806–811.
Ranasinghe, R., Duong, T.M., Uhlenbrook, S., Roelvink, D., Stive, M., 2013. Climate change impact assessment for inlet-interrupted coastlines. Nat. Clim. Chang. 3, 83–87. http://dx.doi.org/10.1038/NCLIMATE1664.
Roelvink, J.A., 2006. Coastal morphodynamic evolution techniques. Coast. Eng. 53, 277–287.
Stive, M.J.F., Capobianco, M., Wang, Z.B., Ruol, P., Buijsman, M.C., 1998. Morphodynamics of a tidal lagoon and the adjacent coast. In: Proceedings of the Eighth International Biennial Conference on Physics of Estuaries and Coastal Seas, The Hague, pp. 397–407.
Tolman, H., 2009. User Manual and System Documentation of WAVEWATCH III™ Version 3.14. NOAA/NWS/NCEP/MMAB Technical Note 276. (194 pp + Appendices, URL http://polar.ncep.noaa.gov/waves/wavewatch/).
University of Moratuwa, 2003. Engineering Study on the Feasibility of Dredging the Negombo Lagoon to Improve Water Quality. Final Report. Part II: Technical & Environmental Feasibility.
van Rijn, L.C., 1993. Principles of sediment transport in rivers, estuaries and coastal seas. Part 1. AQUA Publications, NL (700p).
Wang, Z.B., Jeuken, M.C.J.L., Gerritsen, H., De Vriend, H.J., Kornman, B.A., 2002. Morphology and asymmetry of the vertical tide in the Westerschelde estuary. Cont. Shelf Res. 22, 2599–2609.
Wang, L., Ranasinghe, R., Maskey, S., van Gelder, P.H.A.J.M., Vrijling, J.K., 2015. Comparison of empirical statistical methods for downscaling daily climate projections from CMIP5 GCMs: a case study of the Huai River Basin, China. Int. J. Climatol. http://dx.doi.org/10.1002/joc.4334.
Wijeratne, E.M.S., 2002. Sea Level Measurements and Coastal Ocean Modelling in Sri Lanka. Proceedings of the 1st Scientific Session of the National Aquatic Resources Research and Development Agency, Sri Lanka. (18p).
Zubair, L., Chandimala, J., 2006. Epochal changes in ENSO – streamflow relationships in Sri Lanka. J. Hydrometeorol. 7 (6), 1237–1246.